Comparative Study of Two Low CO_2 Emission Power Generation System Options With Natural Gas Reforming

Na Zhang[1]
Institute of Engineering Thermophysics,
Chinese Academy of Sciences,
Beijing 100080, P.R.C.
e-mail: zhangna@mail.etp.ac.cn

Noam Lior
Department of Mechanical Engineering and
Applied Mechanics,
University of Pennsylvania,
Philadelphia, PA 19104-6315

Two power plant schemes that reduce CO_2 emission and employ natural gas reforming were analyzed and discussed. The first one integrates natural gas reforming technology for efficiency improvement with an oxy-fuel combined power system (OXYF-REF), with water as the main work fluid. The reforming heat is obtained from the available turbine exhaust heat, and the produced syngas is used as fuel with oxygen as the oxidizer. The turbine working fluid can expand down to a vacuum, producing a high-pressure ratio and thus more net work. The second system integrates natural gas reforming in a precombustion decarbonization scheme using chemical absorption technology for the CO_2 removal (PCD-REF). The gas turbine is the conventional air-based one with compressor intercooling. Supplementary combustion is employed to elevate the turbine exhaust temperature and thus achieve a much higher methane conversion rate (96.9%). Both systems involve internal heat recuperation from gas turbine exhausts, and particular attention has been paid to the integration of the heat recovery chain to reduce the related exergy destruction. The systems are simulated and their thermal efficiency, overall and component exergy losses, and CO_2 removal capacity are compared. The OXYF-REF system has a higher energy efficiency, of 51.4%, and higher CO_2 removal, but the product CO_2 has lower purity, of 84%. The PCD-REF system has a thermal efficiency of 46%, the captured CO_2 is 99% pure, and the CO_2 specific emission is 58.5 g/kW h.
[DOI: 10.1115/1.2904895]

1 Introduction

CO_2 separation and sequestration is increasingly regarded as an effective strategy to limit greenhouse gas emissions in fossil-fuel-based power plants. The main three removal strategies are [1–3] (1) postcombustion decarbonization, (2) oxy-fuel power systems, and (3) precombustion decarbonization. Each of these strategies has some relative advantages and disadvantages, and they all decrease power generation efficiency and increase its cost. In this paper, we propose, analyze, and compare two power systems with low CO_2 emissions, employing natural gas reforming technology for fuel conditioning, where one of the systems employs the concepts of an oxyfuel system and the other of precombustion decarbonization, and compare the thermal performance of these two different strategies. To place these systems in the context of CO_2 removal strategies, a brief overview follows.

Postcombustion decarbonization separates CO_2 from the flue gas; it requires minimal modifications to the power system, but large gas quantities must be treated because CO_2 is diluted by the large amounts of nitrogen that are introduced with the combustion air. Chemical absorption of CO_2 is considered to be the most suitable method for this case because of the low CO_2 partial pressure [4].

Oxy-fuel systems are based on close-to-stoichiometric combustion with enriched oxygen and recycled flue gas. The combustion is thus accomplished in the absence of the large amounts of nitrogen, and produces only CO_2 and H_2O. CO_2 separation is accomplished by condensing out the water, typically at ambient temperatures, from the flue gas and therefore requires only a small amount of energy. At the same time, however, a relatively large amount of energy, 7—9% of the total system input, is needed for the oxygen production. The main (and the recycled) working fluid commonly used in the referenced studies is either CO_2 [5–10] or H_2O [11–14]. Also, using CO_2 as the working fluid, we proposed and analyzed semiclosed oxyfuel systems with integration of the LNG (liquefied natural gas) cold exergy utilization [15,16].

To reduce the oxygen production energy efficiency penalty, new technologies have been developed, such as chemical looping combustion (CLC) [17–19] and the advanced zero emissions power plant (AZEP) concept [20,21]. The adoption of these new technologies shows promising performance because no additional energy is then necessary for oxygen separation, but they are still under development [22].

Precombustion decarbonization is accomplished by conversion of the fuel to CO- and H_2-enriched syngas by partial oxidation [1,23] or steam reforming [24,25], followed by a shift process in which CO is converted to CO_2 that is then separated out. Compared to the postcombustion decarbonization from the exhaust, it allows reduced equipment size and lower energy requirements because of much lower quantities of the conditioned gas. Depending on the operational conditions (mainly the pressure and CO_2 concentration), the CO_2 removal can be accomplished by either physical or chemical absorption.

The two low-CO_2 emission power generation systems we propose and analyze in this paper employ natural gas reforming technology for fuel conditioning but with different fuel conversion rates, each having a different improvement objective. In the oxy-fuel semiclosed power system, the steam reforming process is mainly used for the efficiency improvement by turbine exhaust heat recuperation. Similar to that in the chemically recuperated gas turbine (CRGT) cycle [26–28], it utilizes the turbine discharge heat to improve the fuel heating value by producing H_2. Only a

---

[1] Corresponding author.

Contributed by the International Gas Turbine Institute of ASME for publication in the JOURNAL OF ENGINEERING FOR GAS TURBINES AND POWER. Manuscript received October 17, 2007; final manuscript received October 18, 2007; published online June 13, 2008. Review conducted by Dilip R. Ballal.

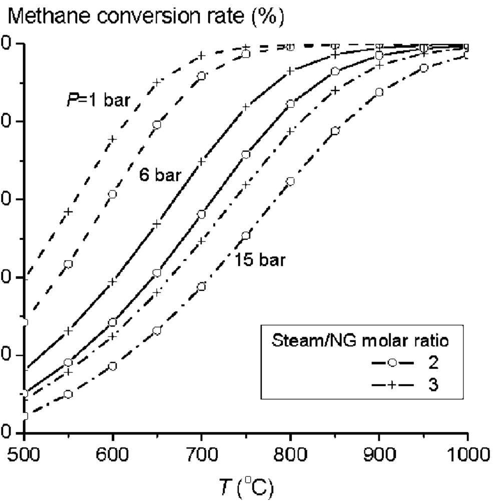

Fig. 1 Methane conversion rate predicted by chemical equilibrium

Table 1 Molar composition and some properties for feed streams

	Natural gas	Oxygen	Air
CH_4 (mol %)	91.18		
C_2H_6 (mol %)	4.41		
C_3H_8 (mol %)	0.1		
N_2 (mol %)	4.31	2	77.3
O_2 (mol %)		95	20.74
CO_2 (mol %)			0.03
H_2O (mol %)			1.01
Ar (mol %)		3	0.92
Temperature (°C)	25	25	25
Pressure (bar)	40	2.38	1.013
Lower heating value (kJ/kg)	46,300	—	
Power consumption for O_2 production (kJ/kg)		812	

medium conversion rate of methane is obtained with the available turbine discharge temperature, and the fact that the CO_2 capture is accomplished by the oxyfuel combustion method is, as explained above, an important advantage. Water vapor is employed as the main working fluid.

In the system with precombustion decarbonization, we employ the steam reforming (together with shift) process for the CO_2 removal. For this reason, supplementary combustion is used to elevate the turbine exhaust temperature and thus allow a much higher precombustion methane conversion rate ($>95\%$) to CO_2. This is intended to minimize the amount of CH_4 that enters the combustor and produces CO_2 emissions from the plant.

In both system configurations, steam is produced by heat recuperation inside the system, both for the reforming process and for combustion injection. The latter increases the working fluid mass flow rate for power generation while demanding very little pumping work for the injected (and then vaporized) water pressure elevation. Particular attention has been paid to the integration of the turbine exhaust heat recovery with both the reforming and the recuperation process.

2 Natural Gas Reforming Process

Chemical recuperation is one of the innovative concepts for improving the performance of natural gas fired gas turbine cycles [26–28]. The natural gas reforming process absorbs heat from the turbine exhaust to produce hydrogen, thus converting some of the turbine exhaust heat into the reforming product heating value.

The reforming process involves the following main reactions [2]:

$$CH_4 + H_2O \leftrightarrow CO + 3H_2 \quad \Delta H = 206.11 \text{ kJ/(mol } CH_4)$$

$$CO + H_2O \leftrightarrow CO_2 + H_2 \quad \Delta H = -41.17 \text{ kJ/(mol CO)}$$

$$C_nH_m + nH_2O \rightarrow nCO + (m/2 + n)H_2$$

The first reaction is the methane reforming. It is highly endothermic and the methane conversion rate is a function of temperature, pressure, and steam/methane ratio, as shown in Fig. 1, which is obtained with ASPEN PLUS software and RK-Soave property method [29], assuming chemical equilibrium, for the natural gas composition given in Table 1.

Low-pressure, high temperature, and high steam consumption increase the reforming conversion. As pointed out by Lozza and Chiesa [25], for power cycles adopting precombustion decarbonization, a methane conversion rate higher than 95% is needed for over 90% CO_2 removal, necessitating large steam consumption and high temperature operation. The typical gas turbine exhaust temperature, 550–600°C, is not sufficiently high for elevated conversion even under low pressure. Therefore, autothermal reforming [23] or supplementary firing [24], in which a fraction of the natural gas is used as fuel, are necessary to increase the turbine exhaust temperature.

The second reaction is known as the shift reaction. In the precombustion decarbonization scheme, the syngas must be shifted as it enriches the CO_2 concentration for CO_2 removal. The third reaction is the reforming of the heavier hydrocarbons contained in the natural gas, which is usually considered irreversible.

The situation is quite different from that in the CRGT cycles, in which turbine exhaust heat is recovered for improving the fuel heating value by methane conversion to H_2 and CO. High conversion of methane is, however, not essential in CRGT because the unconverted reactants are utilized as fuel. In addition, the methane conversion rate is very sensitive to the temperature in the mid-level temperature region (Fig. 1). Supplementary combustion is therefore not essential for the CRGT cycles, in which the fuel conversion is thus based on the available gas turbine exhaust heat and reaches only a moderate level. High methane conversion rate is, as explained above, necessary in the system with precombustion decarbonization we propose because the unconverted CH_4 would otherwise generate CO_2 in the subsequent combustion process.

3 Configuration I: The Oxyfuel System Integrated With Steam Reforming (OXYF-REF)

The conceptual plant configuration analyzed in this section integrates the CRGT concept with oxyfuel combustion [30]. Heat is extracted from the turbine exhaust for reforming with a medium methane conversion rate. An air separation unit is needed to produce oxygen as the combustion oxidizer. CO_2 is removed by water condensation and is subsequently compressed for liquefaction and storage.

The system configuration is shown in Fig. 2. It can be roughly divided into four sections: reforming process (2-3-4-5-6-7-8), power generation, exhaust heat recovery for steam generation (22-23-24-25), and CO_2 compression and liquefaction (28-30).

In the *reforming process section*, the steam and natural gas mixture (State Point 2) (of 2:1 molar ratio) is preheated to (3) by syngas heat recovery and enters the adiabatic reactor PRE-REF, where the heavier hydrocarbons are reformed. The reforming gas temperature drops due to the endothermality of the process (3-4), and it is preheated again before feeding to the reformer REF. The reformer operates at approximately the combustion pressure (~15 bar). It may adopt the conventional counterflow design with the reformer tubes filled with suitable catalyst (such as nickel catalyst pellets) [26]. The cold-side fuel gases flow through this

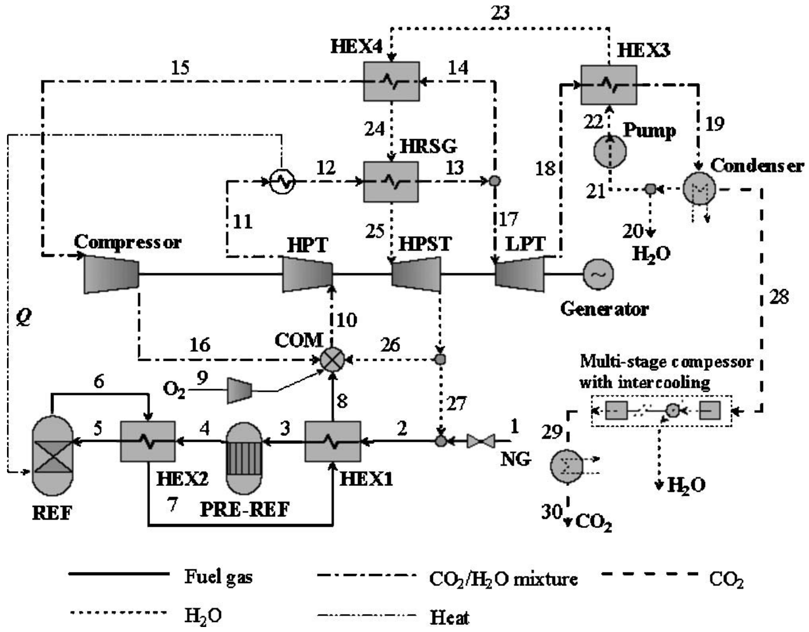

Fig. 2 Process flowsheet of Configuration I: OXYF-REF

packed bed. The heat necessary for reforming is provided by the high-pressure turbine (HPT) exhaust (11-12) flowing on the shell side. Before feeding to the combustor, the syngas (6) is cooled in HEX1 and HEX2 to an assumed maximum temperature of 250°C for preheating the reactants.

The combustion is near stoichiometric with oxygen as the oxidizer. A 2% excess oxygen is assumed. The oxygen is assumed to be produced in a conventional cryogenic vapor compression air separation plant with the specific energy consumption of 812 kJ/kg O_2 [22]. The combustion product is a mixture of mainly CO_2 and H_2O.

The *power generation section* consists of two gas turbines (HPT and LPT), one compressor and one steam turbine (HPST). It can be regarded as a combination of a recuperated oxy-fuel gas turbine cycle with steam injection and a steam Rankine-type cycle. The recuperated gas turbine cycle provides heat (in 11-12 and 12-13) for the reforming process and for steam generation in the HRSG. The steam Rankine cycle recovers the exhaust heat from the gas turbine (GT) cycle and provides steam for both combustion injection (26) and steam reforming (27). The heat recovery section, including HEX3, HEX4, and HRSG, serves as the boiler for the Rankine-like cycle.

The HPT flue gas is divided into two streams (Streams 14 and 17). Stream 14 preheats the Rankine cycle working fluid in HEX4 and then flows to the compressor and combustor of the GT cycle. Stream 17 further expands in LPT to a fairly low-pressure level (0.08 bar in this study), and the water contained is condensed and partly recycled as the Rankine cycle working fluid (21). The configuration of the power generation section is basically similar to the Graz cycle [15]. The arrangement of the higher-pressure (higher heat capacity) but lower mass flow rate fluid on the Rankine cycle side of the heat recovery section, with the lower-pressure (lower heat capacity) but higher mass flow rate fluid on the Brayton cycle side, is for reduction in heat transfer irreversibilities in the heat exchangers.

The combustion-generated CO_2 is separated and compressed to 110 bar (29) in a separate seven-stage compressor with intercooling.

4 Configuration II: The Precombustion Decarbonization Gas Turbine System (PCD-REF)

The GT system with integrated upstream fuel decarbonization and CO_2 removal is shown in Fig. 3. These processes are intended to reduce the amount of carbon entering the combustor and thus of the amount of CO_2 produced in it. Since the CO_2 separation is performed before addition of the oxidant, air can be used without the nitrogen-related energy penalties of postcombustion decarbonization. Basically, it has four main sections too: power generation section, fuel conditioning (reforming and shifting process), CO_2 removal (chemical absorption), and CO_2 compression and liquefaction.

The power generation section consisted of two-stage compressors (LPC and HPC) with intercooling and one GT. Similar in principle to the system proposed by Fiaschi et al. in Ref. [24], it is based on a recuperative GT power cycle with steam injection (8) to the combustor, fueled by the CO_2-free, H_2 enriched, syngas (32). The injected steam is produced by heat recuperation from the compressor intercooling and turbine exhaust. Different from Configuration I in the previous section, the GT uses air (1) as the basic working fluid.

The fuel conditioning chain consists of one reformer (REF) and two-stage shift reactors HTS (high temperature shift reactor) and LTS (low temperature shift reactor). The reformer works at a relatively lower-pressure level (~6 bar) to avoid the need for large steam addition. The GT exhaust temperature is not high enough to obtain a high methane conversion rate. Supplementary combustion (in SC) is thus adopted, which is sustained by excess oxygen in the turbine exhaust (10) and a fraction of the treated syngas (31), to avoid producing CO_2. The turbine exhaust (11-12) with elevated temperature provides heat for the endothermic reaction in REF. The necessary steam is produced by heat recovery inside the fuel conditioning section at the natural gas feed pressure (40 bar). Before feeding to the reformer, the mixture (22) of the produced steam and preheated natural gas (in molar ratio of 2:1) is expanded in the expander to the reformer operation pressure and a temperature of 411°C (23). The produced syngas composition is obtained assuming chemical equilibrium at the REF exit at the

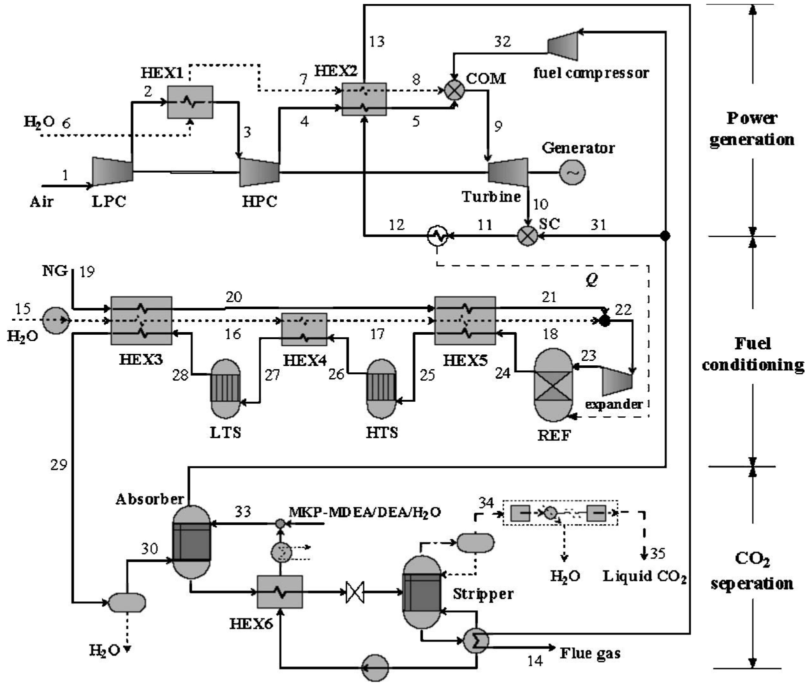

Fig. 3 Process flowsheet of Configuration II: PCD-REF

temperature set at 900°C. Higher steam/natural gas ratios are not considered because more heat would have been needed to be extracted from the turbine exhaust that would have led to lower combustion inlet temperature (Streams 5 and 8) and to less available heat for the amine regeneration. The conversion of CO to CO_2 is advanced in two-stage shift reactions (HTS and LTS). The shift reactions are exothermic and the heat is recuperated for steam generation and natural gas preheating (in HEX3, HEX4, and HEX5). Before being sent to the CO_2 removal section, the syngas (29) is cooled down to near-ambient temperature, and part of the water content is removed by condensation.

The CO_2 *removal section* follows the conventional chemical absorption concept. It consists substantially of an absorber and stripper (regenerator). The solution for CO_2 absorption is a mixture of water and methyl diethanolamine (MDEA) (40% by mass), selected to reduce the reboiler heat duty, as MDEA requires less heat for regeneration than other amines, monoethanolamine (MEA) and diethanolamine (DEA), for example [2]. The rich solution from the absorber is preheated in HEX6 by the lean solution and regenerated in the stripper by extracting heat from the turbine exhaust (13-14) downstream of the recuperator HEX2. The minimal temperature difference in the HEX6 and the reboiler was chosen to be about 10°C. The largely CO_2-free fuel gas from the top of the absorber feeds the combustor and the supplementary combustor (SC). A fuel compressor is necessary to overcome the pressure loss.

The CO_2 *compression and liquefaction section* is the same as that in the OXYF-REF system configuration. The CO_2 enriched gas (34) from the top of the stripper is compressed to 84 bar and liquefied, making liquid CO_2 (35) available for storage.

5 Calculation Assumptions and Method

The proposed systems have all been simulated with the ASPEN PLUS software [29], in which the component models are based on the energy balance and mass balance, with the default relative convergence error (the relative difference between the iteration used and the one before) tolerance of 0.01%. For example, Tables 4 and 5 are the proof of mass balance satisfaction, and Table 6 is the exergy balance. The ELECNRTL and the RK-Soave thermodynamic models were selected for the thermal property calculations for the chemical absorption section and other parts of the systems, respectively. The ELECNRTL property method is the most versatile electrolyte property method. It can handle very low and very high concentrations. It can handle aqueous and mixed solvent systems. It can deal with any liquid electrolyte solution unless there is association in the vapor phase.

The RK-SOAVE property method uses the Redlich–Kwong–Soave (RKS) cubic equation of state for all thermodynamic properties except liquid molar volume. It is recommended for gas-processing, refinery, and petrochemical applications. Example applications include gas plants, crude towers, and ethylene plants. The RK-SOAVE property method can be used for nonpolar or mildly polar mixtures. Examples are hydrocarbons and light gases, such as carbon dioxide, hydrogen sulfide, and hydrogen. This property method is particularly suitable in the high temperature and high-pressure regions, such as in hydrocarbon processing application or supercritical extractions. Reasonable results can be expected at all temperatures and pressures. It is consistent in the critical region, although results are least accurate in the region near the mixture critical point.

The principal reactors (PRE-REF, REF) have been simulated by the Gibbs reactor [2] available in the ASPEN PLUS model library, which determines the equilibrium conditions by minimizing Gibbs free energy. For the chemical absorption section, both absorber and stripper have been simulated using the RadFrac model in the ASPEN PLUS library. Some properties of feed streams are reported in Table 1, and the main assumptions for simulations are summarized in Table 2, and the performance results are reported in Table 3. The calculations use the same natural gas input to provide a common comparison basis.

Some stream state parameters for both system configurations, including temperature, pressure, and composition, are presented in Tables 4 and 5, respectively.

The net system efficiency is defined as

$$\eta=\left[\left(\sum W_T-\sum W_C-\sum W_P-W_{ASU}\right)\eta_{mec}\eta_{gen}\right]/m_f LHV \tag{1}$$

Table 2 Main assumptions for the calculation

Reformer REF	Pressure loss (% of inlet pressure)	5
	Minimum heat transfer temperature difference gas/gas (°C)	23
Prereformer	Pressure loss (% of inlet pressure)	3
Shift reactors	Pressure loss (% of inlet pressure)	2
Compressors	Isentropic efficiency (%)	88
	Fuel and O_2 compressor efficiency (%)	85
Gas turbines	HPT inlet temperature (°C)	1300
	HPT isentropic efficiency (%) (including blade cooling effects)	89
	LPT inlet temperature (°C)	400
	LPT isentropic efficiency (%)	90
	Expander efficiency (%)	85
Steam turbine	HPST inlet pressure (bar)	150
	HPST isentropic efficiency (%)	90
Combustor	Excess O_2 (%) (in the oxyfuel system)	2
	Pressure loss (% of inlet pressure)	3
	Maximum fuel temperature (°C)	250
Heat exchangers	Pressure loss (% of inlet pressure)	1
	Minimum heat transfer temperature difference gas/gas (°C)	20
	Minimum heat transfer temperature difference gas/liquid (°C)	15
Chemical absorption system	Absorber pressure (bar)	5.5
	Stripper pressure (bar)	1.8
	Minimum heat transfer temperature difference (°C)	10
Multistage compressor for CO_2 compression	Number of stages	7
	Stage isentropic efficiency (%)	80
	Intercooler temperature (°C)	35
Pump	Efficiency	85
Ambient state	Temperature (°C)	25
	Pressure (bar)	1.013

$$\varepsilon = \left[\left(\sum W_T - \sum W_C - \sum W_P - W_{ASU}\right)\eta_{mec}\eta_{gen}\right]/A_f \tag{2}$$

$$A_{loss} = \sum A_{in} - \sum A_{out} \tag{3}$$

The exergy dead state is 25°C/1.013 bar.

The system boundary is defined to include all units that contribute to the net system efficiency. In the OXYF-REF system, the process material streams are inflows of fuel (natural gas), and O_2, outflows of pressurized CO_2 and condensed H_2O, and cooling water (in and outflow). In the PCD-REF system, the inflows and outflows across the system boundary include all those mentioned above except the O_2 stream; in addition, the process material streams also include air, the injected water streams for both combustion and reforming, and the flue gas. The energy streams include electricity output and the power consumed for O_2 production (only in the OXYF-REF system). Other energy loss contributors (include mechanical loss and generator loss) are taken into account by assuming a 2% reduction in the gross power output.

Table 3 Performance summary and comparison

Configuration	OXYF-REF	PCD-REF
Natural gas molar flow rate (kmol/h)	3600	3600
Air mass flow rate (kg/s)	—	610
O_2 mass flow rate (kg/s)	68.47	—
Combustor steam injection rate (kg/s)	71.6	59.3
Methane conversion rate (%)	47.12	96.88
Supplementary fuel fraction (%)	—	29.1
HPT power (MW)	548.13	600.36
LPT power (MW)	88.59	—
HPST power (MW)	64.16	—
Expander power (MW)	—	29.98
HPC power (MW)	173.48	135.05
LPC power (MW)	—	99.97
Fuel compressor power (MW)	—	10.93
Water pump power (MW)	1.987	0.166
MDEA pump power (MW)	—	0.244
CO_2 compression power (MW)	36.68	10.64
O_2 production work (MW)	55.59	—
O_2 compression work (MW)	15.31	—
Generator and mech. loss (MW)	8.36	7.47
Net power output (MW)	409.47	365.87
Natural gas *LHV* input (MW)	796.61	796.61
Energy efficiency (%)	51.40	45.93
CO_2 specific emission (g/kW h)	0.0	58.5

6 Exergy Analysis

Using Eqs. (2) and (3), an exergy analysis was performed to examine the exergy losses in all system components, and in the entire system, for obtaining guidance for component and system improvements. The results for the components are shown in Table 6.

Additional information indicating the exergy effectiveness of interactions between heat-exchanging components is obtained by using graphical exergy analysis via the exergy utilization diagram (EUD) method [31]. In this method, an energy donor and an energy acceptor are defined in each energy-transformation/exchange system. For the energy donor and the acceptor, energy change, expressed as the process enthalpy change ΔH, is released by the former and is accepted by the latter, and the corresponding exergy exchange is expressed as

$$\Delta A = \Delta H - T_0 \Delta S \tag{4}$$

They defined the "availability factor" or the "energy level" E as the ratio of the exergy change to the enthalpy (energy) change.

$$E = \Delta A/\Delta H = 1 - T_0(\Delta S/\Delta H) = 1 - \frac{T_0}{T} \tag{5}$$

It is an intensive value and represents the energy quality. We can calculate E for the acceptor and the donor, expressed as E_{ed} and E_{ea}, respectively. By plotting E_{ed} and E_{ea} against the transformed energy ΔH (or Q in a heat exchange process), we obtain the donor-to-acceptor process exergy destruction represented as the area between these curves.

This method has the following advantages: (i) the area between the energy donor and energy acceptor curves, E_{ed} and E_{ea}, represents a characteristic feature of each process equal to the exergy destruction of the corresponding section of the system, and (ii) the energy-level difference ($E_{ed}-E_{ea}$) represents the driving force to make the process proceed. When its value becomes the smallest, a pinch point is found at that location.

The E-Q (ΔH) diagrams of some key processes are shown in Figs. 4 and 5. It should be pointed out that the system configurations and operating parameters are not necessarily optimal for each system. A few comments that are valid for the chosen configurations and parameters can be made on the exergy analysis results.

- While the natural gas input exergy A_f was chosen to be the same for both systems (taken as 100%), the OXYF-REF system contains an additional 1.33% amount of exergy input contained in the O_2 stream from the *ASU*.
- On the output side, it is also noteworthy that the pressurized CO_2 streams separated from each system possess exergy (corresponding to the reversible work that could have been produced by isothermal expansion of the pressurized CO_2 to its partial pressure in the environment) amounting to 4.9% and 4.4% of A_f for Systems I and II, respectively. If we consider the captured high-pressure CO_2 stream also as an exergy-valuable product of the system, the total exergy efficiencies would be 53.5% and 47.8% for these two systems.
- The combustion-associated exergy loss is, as usual, the highest loss, amounting to 26.6% in the OXYF-REF system

Table 4 Main stream states of the OXYF-REF system (the state point numbers refer to Fig. 2)

No.	T (°C)	P (bar)	m (kg/s)	Molar composition (%)								
				CH_4	C_2H_6	H_2	CO	CO_2	H_2O	O_2	N_2	Ar
Reforming section												
2	192.3	16.95	53.24	30.4	1.5				66.7		1.4	
3	550	16.8	53.24	30.4	1.5				66.7		1.4	
4	453.8	16.35	53.24	28.7		9.9	0.1	2.8	57.2		1.4	
5	639.7	16.2	53.24	28.7		9.9	0.1	2.8	57.2		1.4	
6	740	15.6	53.24	11.9		43.8	6.6	6.3	30.3		1.1	
8	250.3	15.45	53.24	11.9		43.8	6.6	6.3	30.3		1.1	
Power generation section												
10	1300	15	471.06					11	86.9	0.4	0.9	0.7
11	763.4	1.05	471.06					11	86.9	0.4	0.9	0.7
12	649.3	1.04	471.06					11	86.9	0.4	0.9	0.7
17	400	1.03	193.32					11	86.9	0.4	0.9	0.7
18	134.3	0.082	193.32					11	86.9	0.4	0.9	0.7
25	620.8	150	107.62						100			
26	292	16.95	71.59						100			
CO_2 compression												
28	35	0.08	74.29					39.8	52.7	1.6	3.4	2.5
29	35	110	50.40					84	0.2	3.3	7.2	5.3

and to 29.2% of A_f in the PCD-REF system. The higher latter loss is because (cf. Ref. [32]) one of the two combustors, SC, operates at a lower temperature than the combustor in the former system and because the mass flow rate through the combustors in the latter system is higher.

- The reforming section includes the reactors and the heat exchangers. The syngas heat is largely recuperated internally by preheating the reactants. The EUDs in the reforming section are shown in Figs. 4(*a*) and 4(*b*), and the exergy loss represented by the shaded area is obviously larger in the PCD-REF system. In the OXYF-REF system, the reformer has two sections: the adiabatic section 5-5′ and endothermic section 5′-6. The reaction in PRE-REF is also adiabatic, with limited conversion rate. The adiabatic reactions in both PRE-REF (3-4) and REF (5-5′) each are designed to undergo a temperature drop of nearly 100 °C to allow the turbine exhaust to be cooled to a low value, so that to increase both the exhaust heat recovery for reforming and the final reforming temperature. The exergy loss is found to be 16.8 MW, which is about 2% of the natural gas input exergy A_f. In the PCD-REF system, the reforming process requires a higher heat input because of the high reforming temperature of 900 °C. Compared to 107 MW in the OXYF-REF configuration, the heat duty of REF is 286 MW here, leading to larger exergy loss in REF. The syngas heat is recuperated by feedwater and natural gas preheating in HEX3, HEX4, and HEX5 that are included in the reforming section

Table 5 Main stream states of the PCD-REF system (the state point numbers refer to Fig. 3)

No.	T (°C)	P (bar)	m (kg/s)	Molar composition (%)								
				CH_4	C_2H_6	H_2	CO	CO_2	H_2O	O_2	N_2	Ar
Power generation section												
1	25	1.013	610					0.03	1.0	20.7	77.3	0.9
5	600	15.45	610					0.03	1.0	20.7	77.3	0.9
8	600	15.45	59.3						100			
9	1300	15	679.03					0.3	24.3	11.5	63.1	0.7
10	658.8	1.06	679.03					0.3	24.3	11.5	63.1	0.7
11	935.2	1.04	683.03					0.4	28.1	9.1	61.7	0.7
12	633	1.03	683.03					0.4	28.1	9.1	61.7	0.7
13	233.2	1.02	683.03					0.4	28.1	9.1	61.7	0.7
14	124	1.013	683.03					0.4	28.1	9.1	61.7	0.7
Fuel conditioning section												
22	629.4	40	53.24	30.4	1.5				66.7		1.4	
23	410.9	6.3	53.24	30.4	1.5				66.7		1.4	
24	900	6.1	53.24	0.6		61.5	16.3	3.4	17.3		0.9	
26	493.9	5.95	53.24	0.6		69.7	8.1	11.5	9.2		0.9	
28	256.9	5.8	53.24	0.6		77.4	0.4	19.3	1.4		0.9	
CO_2 removal section												
30	35	5.7	52.63	0.6		78	0.4	19.4	0.8		0.9	
31	48.8	5.5	4.0	0.6		94.5	0.5	1.4	2		1.1	
32	178.7	15.45	9.73	0.6		94.5	0.5	1.4	2		1.1	
34	35	1.8	38.79	0.4				96.3	3.2		0.1	
35	35	83.69	38.35	0.4				99	0.5		0.1	

Table 6 Exergy analysis results and comparison

	OXYF-REF		PCD-REF	
Configuration	MW	%	MW	%
Exergy input				
Natural gas	843.41	100	843.41	100
O_2 feed stream	11.25	1.33		
Exergy output				
Net power output	409.5	48.55	365.87	43.38
Energy for O_2 production	55.59	6.59		
CO_2 stream	41.48	4.92	37.42	4.44
Exergy loss				
Combustor	224.01	26.56	245.88	29.15
Reforming process	16.83	2.0	41.93	4.97
Turbine HPT/LPT/ST/expander	31.62	3.75	27.23	3.23
Compressors (including O_2 compressor)	9.99	1.18	17.08	2.03
Heat exchangers[a]	43.11	5.11	27.64	3.28
Chemical absorption	—	—	33.57	3.98
CO_2 compression	15.49	1.84	3.52	0.42
Flue gas	—	—	35.05	4.16
Mechanical and generator losses	8.36	0.99	7.47	0.89

[a] HEX1, HEX2 and HRSG in OXYF-REF; HEX1 and HEX2 in PCD-REF

too, to reduce the HTS and LTS inlet temperatures to 400 °C and 160 °C. As shown in Fig. 4(*b*), the exergy loss in HEX5 is relatively large because of the poor thermal match with the isothermal steam evaporation process. The total exergy loss in the reforming process is 41.9 MW, accounting for 5% of the natural gas input exergy A_f. As indicated by the EUD, a way to reduce the exergy losses is to reduce the difference between E_{ed} and E_{ea}. Smaller $(E_{ed} - E_{ea})$ means a closer match between the energy donor and acceptor. In a heat exchange process, this would be accomplished by choosing a smaller average heat transfer temperature difference, which also leads to the need for larger heat transfer area or/and higher heat transfer coefficients and thus higher cost.

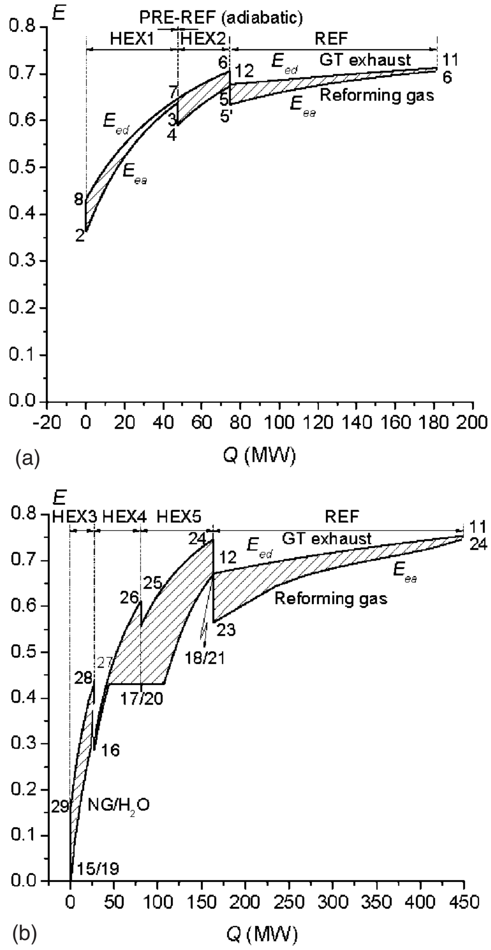

Fig. 4 (*a*) EUD in the reforming section of the OXYF-REF cycle and (*b*) EUD in the reforming section of the PCD-REF cycle

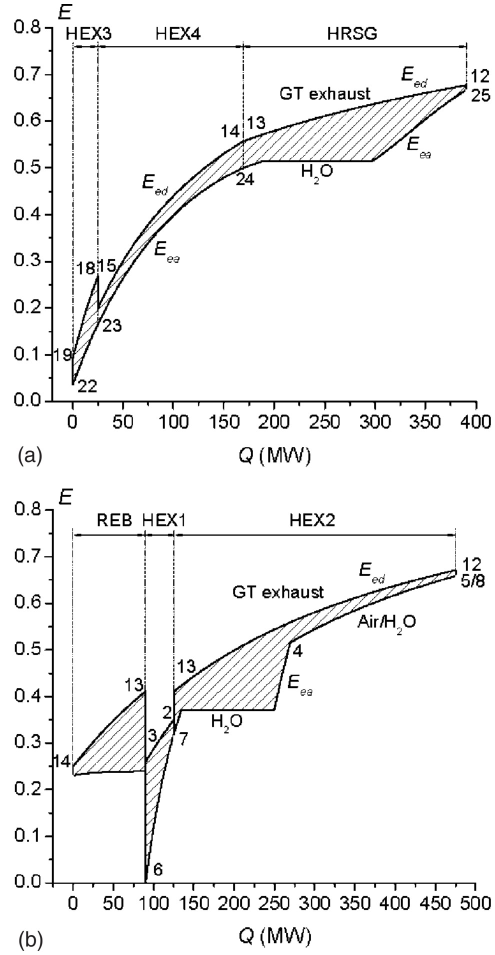

Fig. 5 (*a*) EUD in the turbine exhaust heat recovery process of the OXYF-REF cycle and (*b*) EUD in the heat recovery process of the PCD-REF cycle

- We now examine the exergy losses in the heat recovery sections, composed of several heat exchangers, of both systems. In the OXYF-REF system, Fig. 5(*a*) is the EUD of the water preheating and steam generation process in HEX3, HEX4, and HRSG, and the related exergy loss was computed to be about 43 MW, 5.1% of the total natural gas exergy input. Part of the HPT flue gas is directly recycled (at Point 14 in Fig. 2) to the compressor and then to the combustor, its sensible heat is mainly utilized to preheat water (in HEX4), and this also helps to reduce the compressor power consumption; therefore, the recycle fraction (m_{14}/m_{13}) is determined by the heat demand of the water side considering the minimal heat transfer temperature difference, and it also has influence on the compressor power consumption and the turbine power output. The recycled fraction is found to be 59% in this calculation, which means

Table 7 The CO_2 enriched mixture composition after the multistage compression

Configuration	State point	T (°C)	P (bar)	Vapor fraction	Mass flow rate (kg/s)/molar composition (%)					
					CH_4	CO_2	H_2O	O_2	N_2	Ar
OXYF-REF	29	35	110	1		44.14/84	0.037/0.2	1.27/3.3	2.4/7.2	2.55/5.3
PCD-REF	35	35	83.7	0	0.062/0.4	38.19/99	0.079/0.5		0.013/0.1	

that the working fluid mass flow rate of LPT is 41% of that of HPT.

In the PCD-REF system, besides providing heat for the reforming and recuperation (in HEX2), the turbine exhaust also sustains the reboiler heat duty. The reformer REF, the recuperator HEX2, and the reboiler are configured in a cascade according to the temperature levels, intending also to reduce the heat transfer related exergy destruction. The reformer is upstream of the SC exhaust, taking advantage of the possibly highest temperature available (11-12). The recuperator HEX2 produces steam for combustion injection and also preheats the combustion air (and steam) to 600 °C. The steam injection rate (the mass flow rate ratio between the injected steam and the compressor inlet air) is 9.7% in this calculation. Larger steam injection is favorable to the global energy efficiency, but would lead to less heat available to the reboiler.

Downstream the cascade, the exhaust heat (13-14) is used for regeneration of amine in the CO_2 removal section. The exhaust gas enters the reboiler at 233 °C and leaves at 124 °C, providing 90.2 MW heat for the amine regeneration. The exhaust heat recovered percentages in REF, HEX2 and the reboiler are 39.4%, 48.2%, and 12.4%, respectively.

Figure 5(*b*) is the EUD for the reboiler REB, HEX1, and HEX2 in system PCD-REF. The match between the isothermal heat sink of steam evaporation and the sensible heat resource of GT exhaust gas leads to relatively large exergy loss (23.2 MW) in HEX2. The total exergy losses in HEX1 and HEX2 are found to be 27.6 MW, accounting for 3.3% points of the fuel exergy input A_f. As mentioned before, the exergy loss in the heat exchangers can be reduced with smaller ($E_{ed}-E_{ea}$). This can be accomplished by parameter optimization or rearrangement of the match between the energy donor and acceptor (configuration optimization).

- In the power generation section, the turbine related exergy loss is 31.6 MW in the OXYF-REF system, slightly larger than that in the PCD-REF system, because of the higher power output. However, the compressor-related exergy loss in the PCD-REF system is 7 MW larger than that in the OXYF-REF system because more working fluid is treated, resulting in higher compression work demand. The turbine and compressor exergy loss can be reduced if more efficient components are employed.
- In the OXYF-REF system, about 55.6 MW power (6.6% of the natural gas exergy input) is used for O_2 production, and this is treated as an exergy outflow from the system.
- The PCD-REF system employs a chemical absorption section for CO_2 removal. The related exergy loss includes the absorption, amine regeneration (in REB), heat exchange, and the remaining processes, and is found to be 33.6 MW, accounting for 4% of the total exergy input. The turbine flue gas exhausts (State 14) at a temperature of 124 °C, after providing heat to the reboiler, lead to a 35 MW (4.2% of A_f) loss to the environment. The relatively high exhaust temperature is mandated by the heat transfer temperature difference in REB. The flue gas exergy loss can be reduced by further utilization of the exhaust heat for heat production.

7 Overall Performance Comparison and Discussion

We recall now that the two system configurations differ in several ways, basically based on the different CO_2 removal strategies (Table 7). OXYF-REF and PCD-REF have, respectively,

- different working fluids: the mixture of H_2O/CO_2 and air
- different system configurations in the power generation section: a combined gas/steam cycle and a recuperated GT cycle
- different operation parameters: most notably different REF operation conditions and different turbine exhaust conditions, where in the OXYF-REF system, the turbine working fluid can expand down to a vacuum, significantly enlarging the overall working pressure region

7.1 Power Generation Section. The OXYF-REF system has a net power output of 409.5 MW, with an energy efficiency of 51.4%. Most of the power (78.2%) is generated by the HPT GT. The compressor consumes more power than that produced by the LPT and HPST turbines.

The CO_2 multistage compressor power demand is 36.7 MW, which is much higher than that for the PCD-REF system, because of the larger amount of the gases compressed and the presence of a large quantity of noncondensable gases.

The energy consumption for O_2 production and compression is 70.9 MW, which accounts for 8.9% of the total system energy input.

The PCD-REF system has a net power output of 365.9 MW, lower by about 10.6% than that of the OXYF-REF system, largely because only 71% of the fuel gas feeds the combustor, with the remaining 29% used for the SC needed to support the reforming, resulting in an overall energy efficiency of 45.9%. This efficiency is higher by ~3% points than the efficiency reported in Ref. [24] for a similar recuperative GT cycle but with atmospheric pressure reforming, and approaches the 46%–48% efficiencies reported for the gas/steam combined cycle configurations proposed in other studies [1,2,25]. As to the PCD-REF system, it is noteworthy that it can be regarded as a combined gas/steam turbine cycle (since steam is injected into the combustor) with some of its advantages but having a much simpler configuration.

7.2 Fuel Conditioning Section. The methane conversion rate depends on the reforming conditions. The reformers work at different pressures and temperatures in each of the two systems, but with the same steam/natural gas molar ratio. In the OXYF-REF system, the reformer products exit at a temperature of 740 °C, restricted by the turbine exhaust temperature (which is higher than that of the conventional air-based GT exhaust because of the different working fluids). It achieves a medium methane conversion rate of 47.1%. The syngas molar compositions are 43.8% H_2, 6.3% CO_2, 6.6% CO, 11.9% CH_4, and 30.3% H_2O. The CO_2 and H_2O compositions were then elevated to 11% and 87% by combustion in COM.

In the PCD-REF system configuration, a methane conversion rate of 96.9% is achieved, the high value attributed to lower reforming pressure and the supplementary combustion in SC. Such supplementary combustion typically has a negative effect on the

Table 8 Main results for the CO_2 removal section in the PCD-REF system

Solvent mass flow rate (kg/s)	500
Reboiler heat duty (MW)	90.2
Absorber feed CO_2 (kg/s)/(mol %)	42/19.4
CO_2 in the fuel gas (kg/s)/(mol %)	2.43/1.4
CO_2 in distillate (kg/s)	38.19
Removal efficiency (%)	90.9

overall efficiency because the associated supplementary fuel energy is not fully exploited for power production and is used only at a lower temperature level. In this analysis, this supplementary fuel fraction is 29%. 97.5% of CO in the syngas was converted to CO_2 after the two-stage shift process. Compared to the first configuration, the syngas after CO_2 removal is much more enriched in H_2 (with a molar fraction of 94.5%), leading to a very high heating value of this clean fuel.

7.3 CO_2 Removal/Compression Section. In the multistage CO_2 compressor, water is removed after each stage of intercooling. In the OXYF-REF system, the captured CO_2 stream is a gaseous mixture at 110 bar/35 °C. In the PCD-REF system, the captured CO_2 stream is in the liquid state already at 84 bar/35 °C.

As shown in Table 7, the CO_2 volume content in the OXYF-REF system configuration is 84%; the O_2, N_2, and Ar amount to 15.8%, mainly depending on the oxygen purity, natural gas composition, and the excess oxygen rate beyond the stoichiometric combustion. Further purification might be required to remove some of the gas components prior to transportation and storage. According to Ref. [22], purifying CO_2 would incur a power cycle efficiency reduction up to 0.4% points and would add to the overall cost. Davison [33] mentioned an oxy-fuel natural gas fired combined cycle plant in which the flue gas with a CO_2 concentration of 88 mol % dry basis is compressed and the CO_2 concentration is increased to 96 mol % by a cryogenic unit for removal of inert gases that is integrated with the compression unit. In this paper, the mixture is compressed to 110 bar, and the presence of the noncondensable species increases the compression power requirement. Further purification and its effect were not taken into consideration, and the calculation indicates that the pressurized stream can be liquefied at a near-ambient temperature of 16.5 °C. Assuming 100% capture, the final liquid pure CO_2 mass flow rate is 44.1 kg/s. However, a trace amount of CO_2 will in any case be dissolved in the water.

In the PCD-REF system configuration, the CO_2 molar composition of the absorber feed stream is 19.4% and reduced to 1.4% in the fuel gas after CO_2 removal. The removal efficiency of the chemical absorption is 90.9% (Table 8), and it increases by increasing the heat input to the reboiler. The actual captured CO_2 of 38.2 kg/s is 86.5% of that in the OXYF-REF system. The total CO_2 emission (does not include those introduced with air) in the flue gas plus those escaped from the chemical absorption is 5.95 kg/s, making the specific emission of 58.5 g/kW h, compared, e.g., to 41–43 g/kW h reported in Refs. [1,2,25] with combined cycle configurations and 155 g/kW h in Ref. [24] adopting a recuperative GT cycle. It is noticed that 13.6% of the unconverted CH_4 (mass flow rate of 0.062 kg/s) was removed together with CO_2 in the chemical absorption plant, which takes account of ~0.4% of the total CH_4 input to the system. This fraction of CH_4 will be released during the CO_2 liquefaction process and is lost for both power generation and CO_2 capture. Since methane has a greenhouse effect that is 20–30 times higher than that of CO_2 for the same concentration, it is important to minimize its release to the atmosphere. Methane emissions in the proposed systems are, however, not higher than methane emissions from any other power generation system that uses methane as fuel and chemical absorption for CO_2 capture.

7.4 Technology Considerations. The hardware challenge associated with the oxyfuel system is mainly the CO_2/H_2O turbine. The mixture of CO_2/H_2O has different expansion characteristics than the combustion gas in conventional GTs, resulting in higher exhaust temperatures for the same pressure ratio and turbine inlet temperature. The optimal pressure ratio is also higher than that for the air-based turbines. The CO_2/H_2O turbine calls for a new design since the existing turbines cannot be easily adapted to the new working fluid.

The combustor is another technological challenge for both the oxyfuel system and the one with precombustion decarbonization. For the oxyfuel system, it involves the combustion in a pure oxygen environment. A review about the oxyfuel combustion technology was given in Ref. [34] but focused on coal based systems. Another one by Pronske et al. [35] summarized the development of oxyfuel turbine and combustor technology by the Clean Energy Systems (CES) company and Siemens Power Generation for the 300–600 MW coal syngas plant with zero emissions.

For the precombustion capture plant with reforming, the major problem of the combustor is NO_x emission control when burning hydrogen-enriched fuel, which has very high heating value and flame temperature. Premixed combustion is difficult to apply for hydrogen combustion due to its high reactivity. Some studies suggested that fuel dilution with steam or nitrogen, accompanied with certain efficiency loss, might be a feasible solution [36].

The technological difficulties are different for the reformers in the two configurations. In the environments containing carbon and hydrogen compounds in the critical temperature range of about 400–800°C, metal dusting can potentially be a severe corrosion problem [37]. Some known techniques to minimize the effects of metal dusting include additional steam injection and preoxidation to build and maintain a stable, adherent, healable oxide surface layer on the exposed metal surfaces. In the OXYF-REF system, the reformer is susceptible to metal dusting because it produces syngas at the temperature of 740°C, which may necessitate the use of materials that exhibit good resistance to metal dusting attack. The metal dusting is avoided in the PCD-REF configuration by designing the operation to take place above the critical temperature range. However, the high temperature reformer in the PCD-REF configuration may cause some technological difficulties too, mainly the material stress, operation lifetime and cost, etc. In this study, the temperature above 900°C is used to obtain a desired conversion rate with limited steam addition. The pressurized reforming process is used, and it allows reduced equipment size. Considering the great influence of the pressure on performance and hardware, a thermoeconomic comparison with an atmospheric reforming process would be useful.

Another technological issue in the PCD-REF system is associated with the entrainment of amine traces (MDEA) by the clean synfuel, which may be corrosive to the turbine blades and combustor. The calculation results from ASPEN PLUS indicate that the residual MDEA mass fraction in the clean fuel is 2 ppm. The negative effect of such a small amount is assumed in this study to be negligible; so, further processes/equipment for removing these trace amounts were not considered. Prevention of the amine contamination requires an adequate design of the amine droplet separation system, as addressed in Refs. [23,24].

8 Concluding Remarks

Steam reforming is an effective strategy for CO_2 capture from natural gas fuel power plants. Chemical recuperation for fuel conversion is also considered to result in higher plant efficiency than the conventional physical recuperation with heat transfer.

The paper presented two novel systems that integrate steam reforming, one with oxyfuel cycle technology that eliminates air-N_2 input to the GT working fluid and thus allows simple separation of the CO_2 from its exhaust, and the other with precombustion decarbonization technology employing chemical absorption, for CO_2 removal in natural gas fired power plants. The two systems were then thermodynamically simulated and compared. To increase efficiency, they both employ high temperature internal combustion, with steam injection into the combustor.

Considering that 100% of the CO_2 was captured, the OXYF-REF system is better in that respect than the PCD-REF one, but the captured CO_2 is mixed with other gases, and emerges in gaseous state at a concentration of 84%. Additional energy would hence be necessary for its further purification and liquefaction, and the penalty to the overall efficiency is estimated to be 0.4% points in Ref. [22]; this effect is not considered in this analysis. The PCD-REF has a 58.5 g/kW h specific CO_2 emission, achieving 86.5% CO_2 removal that is thus lower than the 100% removal for the oxyfuel system. The captured CO_2 is, however, at high purity of 99% and in liquid state. In PCD-REF, 10% of the uncaptured CO_2 escapes with the flue gas and 3% remains unseparated from the amine during the stripping process using the reboiler. In this calculation, the reboiler heat demand is fully sustained by the turbine exhaust heat recovery and is restricted by the minimal temperature difference in the reboiler.

The PCD-REF system, which employs a recuperated GT cycle, has a global energy efficiency lower by 5.4% points than that found for the OXYF-REF combined system, mainly due to additional fuel demand for the supplementary firing. Its efficiency of 46% is, however, comparable to some other systems employing a combined gas/steam cycle configuration.

As to the hardware requirement, the OXYF-REF system includes an air separation unit, consuming about 7% of the total system energy input. It also employs an additional turbine, a HP steam turbine for additional power generation. The PCD-REF system employs a more complicated fuel conditioning section with two-stage shift reactors and a chemical absorption unit for CO_2 removal. It achieves the energy efficiency of around 46% without inclusion of a closed steam cycle (thus eliminating steam turbine, condenser, and associated hardware). An economic analysis was not performed but is obviously necessary for a more comprehensive comparison.

The turbine exhaust heat is largely recuperated internally in both configurations. The heat recovery chains were carefully arranged to reduce the heat transfer related exergy destruction. An exergy analysis was performed to examine the exergy losses in all system components and in the entire system, also with the aid of the EUD method, for obtaining guidance for component and system improvements. It is found that the system exergy efficiencies (based on the electricity generated) are 48.6% for OXYF-REF and 43.4% for PCD-REF. The OXYF-REF system has lower exergy losses in both the combustion and reforming processes, but the O_2 production energy consumption is 6.6% of the fuel exergy input. Comparatively, the PCD-REF system has an additional exergy loss of 4% of A_f in the chemical absorption process and also has a flue gas related exergy loss of 4.2% of A_f.

Acknowledgment

The senior author gratefully acknowledges the support of the National Natural Science Foundation of China Project (No. 50520140517).

Nomenclature

A = exergy (kW)
E = $\Delta A/\Delta H$, Eq. (5)
H = enthalpy (kW)
LHV = lower heating value (kJ/kg)
m = mass flow rate (kg/s)
P = pressure (bar)
T = temperature (°C)
Q = heat duty (MW)
W = power (MW)
ε = exergy efficiency (%)
η = energy efficiency (%)

Subscripts

0 = ambient state
1,2,…,35 = states on the cycle flow sheet
ASU = air separation unit
C = compressor
ea = energy acceptor
ed = energy donor
f = fuel
gen = generator
in = inlet
mec = mechanical
out = outlet
P = pump
T = turbine

Component

COM = combustor
HEX = heat exchanger
HPC = high-pressure compressor
HPST = high-pressure steam turbine
HPT = high-pressure gas turbine
HRSG = heat recovery steam generator
HTS = high temperature shift reactor
LPC = low-pressure compressor
LPT = low-pressure gas turbine
LTS = low temperature shift reactor
PRE-REF = prereformer
REF = reformer

References

[1] Lozza, G., and Chiesa, P., 2002, "Natural Gas Decarbonization to Reduce CO_2 Emission From Combined Cycles—Part I: Partial Oxidation," ASME J. Eng. Gas Turbines Power, **124**, pp. 82–88.

[2] Corradetti, A., and Desideri, U., 2005, "Analysis of Gas-Steam Combined Cycles With Natural Gas Reforming and CO_2 Capture," ASME J. Eng. Gas Turbines Power, **127**, pp. 545–552.

[3] Chiesa, P., and Consonni, S., 2000, "Natural Gas Fired Combined Cycles With Low CO_2 Emissions," ASME J. Eng. Gas Turbines Power, **122**, pp. 429–436.

[4] Desideri, U., and Paolucci, A., 1999, "Performance Modeling of a Carbon Dioxide Removal System for Power Plants," Energy Convers. Manage., **40**, pp. 1899–1915.

[5] Mathieu, P. and Nihart, R., 1999, "Zero-Emission MATIANT Cycle," ASME J. Eng. Gas Turbines Power, **121**, pp. 116–120.

[6] Mathieu, P. and Nihart, R., 1999, "Sensitivity Analysis of the MATIANT Cycle," Energy Convers. Manage., **40**, pp. 1687–1700.

[7] Yantovski, E. I., Zvagolsky, K. N., and Gavrilenko, V. A., 1996, "The COOPERATE—Demo Power Cycle," Energy Convers. Manage., **37**(6–8), 861–864.

[8] Yantovski, E. I., 1996, "Stack Downward Zero Emission Fuel-Fired Power Plants Concept," Energy Convers. Manage., **37**, pp. 867–877.

[9] Staicovici, M. D., 2002, "Further Research Zero CO_2 Emission Power Production: The "COOLENERG" Process," Energy, **27**, pp. 831–844.

[10] Bolland, O., and Mathieu, P., 1998, "Comparison of Two CO_2 Removal Options in Combined Cycle Power Plants," Energy Convers. Manage., **39**, pp. 1653–1663.

[11] Anderson, R., Brandt, H., Doyle, S., Pronske, K., and Viteri, F., 2003, "Power Generation With 100% Carbon Capture and Sequestration," Second Annual Conference on Carbon Sequestration, Alexandria, VA.

[12] Marin, O., Bourhis, Y., Perrin, N., Zanno, P. D., Viteri, F., and Anderson, R., 2003, "High Efficiency, Zero Emission Power Generation Based on a High-Temperature Steam Cycle," 28th International Technical Conference on Coal Utilization and Fuel Systems, Clearwater, FL.

[13] Jericha, H., Gottlich, E., Sanz, W., and Heitmeir, F., 2004, "Design Optimization of the Graz Cycle Prototype Plant," ASME J. Eng. Gas Turbines Power, **126**, pp. 733–740.

[14] Martinez-Frias, J., Aceves, S. M., Smith, J. R., and Brandt, H., 2004, "Thermodynamic Analysis of Zero-Atmospheric Emissions Power Plant," ASME J. Eng. Gas Turbines Power, **126**, pp. pp.2–8.

[15] Zhang, N. and Lior, N., 2006, "A Novel Near-Zero CO_2 Emission Thermal Cycle With LNG Cryogenic Exergy Utilization," Energy, **31**, pp. 1666–1679.

[16] Zhang, N. and Lior, N., 2006, "Proposal and Analysis of a Novel Zero CO_2 Emission Cycle With Liquid Natural Gas Cryogenic Exergy Utilization," ASME J. Eng. Gas Turbines Power, **128**, pp. 81–91.

[17] Ishida, M., and Jin, H., 1997, "CO_2 Recovery in a Novel Power Plant System With Chemical-Looping Combustion," Energy Convers. Manage., **38**(19), pp. 187–192.

[18] Ishida, M., and Jin, H., 1994, "A New Advanced Power-Generation System Using Chemical-Looping Combustion," Energy, **19**, pp. 415–422.

[19] Naqvi, R., and Bolland, O., 2005, "Off-Design Evaluation of a Natural Gas Fired Chemical Looping Combustion Combined Cycle With CO_2 Capture," *Proceedings of ECOS2005*, Trondheim, Norway, pp. 827–834.

[20] Griffin, T., Sundkvist, S. G., Asen, K., and Bruun, T., 2005, "Advanced Zero Emissions Gas Turbine Power Plant," ASME J. Eng. Gas Turbines Power, **127**, pp. 81–85.

[21] Moller, B. F., Torisson, T., Assadi, M., Sundkvist, S. G., Sjodin, M., Klang, A., Asen, K. I., and Wilhelmsen, K., 2005, "AZEP Gas Turbine Combined Cycle Power Plants—Thermo-Economic Analysis," *Proceedings of ECOS2005*, Trondheim, Norway, pp. 819–826.

[22] Kvamsdal, H. M., Jordal, K., and Bolland, O., 2007, "A Quantitative Comparison of Gas Turbine Cycles With CO_2 Capture," Energy, **32**, pp. 10–24.

[23] Fiaschi, D., Lombardi, L., and Tapinassi, L., 2003, "The Recuperative Auto Thermal Reforming and Recuperative Reforming Gas Turbine Power Cycles With CO_2 Removal—Part I: The Recuperative-Auto Thermal Reforming Cycle," ASME J. Eng. Gas Turbines Power, **125**, pp. 933–939.

[24] Fiaschi, D., Lombardi, L., and Tapinassi, L., 2004, "The Recuperative Auto Thermal Reforming and Recuperative Reforming Gas Turbine Power Cycles With CO_2 Removal—Part II: The Recuperative Reforming Cycle," ASME J. Eng. Gas Turbines Power, **126**, pp. 62–68.

[25] Lozza, G., and Chiesa, P., 2002, "Natural Gas Decarbonization to Reduce CO_2 Emission From Combined Cycles—Part II: Steam-Methane Reforming," ASME J. Eng. Gas Turbines Power, **124**, pp. 89–95.

[26] Adelman, S. T., Hoffman, M. A., and Baughn, J. W., 1995, "A Methane-Steam Reformer for a Basic Chemically Recuperated Gas Turbine," ASME J. Eng. Gas Turbines Power, **117**, pp. 16–23.

[27] Abdallah, H., Facchini, B., Danes, F., and De Ruyck, J., 1999, "Exergetic Optimization of Intercooled Reheat Chemically Recuperated Gas Turbine," Energy Convers. Manage., **40**, pp. 1679–1686.

[28] Kesser, K. F., Hoffman, M. A., and Baughn, J. W., 1994, "Analysis of a Basic Chemically Recuperated Gas Turbine Power Plant," ASME J. Eng. Gas Turbines Power, **116**, pp. 277–284.

[29] ASPEN PLUS®, Aspen Technology, Inc., Version 11.1, http://www.aspentech.com/, Aspen Physical Property System, Physical Property Methods and Models 11.1, Sept. 2001, Aspen Technology, Inc., Cambridge, MA.

[30] Zhang, N., and Lior, N., 2006, "Configuration Analysis of Oxy-Fuel Cycles With Natural Gas Reforming and CO_2 Capture," *Proceedings of ECOS2006*, Crete, Greece, pp. 1619–1628.

[31] Ishida, M., and Kawamura, K., 1982, "Energy and Exergy Analysis of a Chemical Process System With Distributed Parameters Based on the Energy-Direction Factor Diagram," Ind. Eng. Chem. Process Des. Dev., **21**, pp. 690–695.

[32] Dunbar, W. R., and Lior, N., 1994, "Sources of Combustion Irreversibility," Combust. Sci. Technol., **103**, pp. 41–61.

[33] Davison, J., 2007, "Performance and Cost of Power Plants With Capture and Storage of CO_2," Energy, **32**, pp. 1163–1176.

[34] Buhre, B. J. P., Elliott, L. K., Sheng, C. D., Gupta, R. P., and Wall, T. F., 2005, "Oxy-Fuel Combustion Technology for Coal-Fired Power Generation," Prog. Energy Combust. Sci., **31**, pp. 283–307.

[35] Pronske, K., Trowsdale, L., Macadam, S., Viteri, F., Bevc, F., and Horazak, D., 2006, "An Overview of Turbine and Combustor Development for Coal-Based Oxy-Syngas System," ASME Paper No. GT2006-90816.

[36] Damen, K., Troost, M., Faaij, A., and Turkenburg, W., 2006, "A Comparison of Electricity and Hydrogen Production Systems With CO_2 Capture and Storage. Part A: Review and Selection of Promising Conversion and Capture Technologies," Prog. Energy Combust. Sci., **31**, pp. 215–246.

[37] Hazeldine, P., and Baker, B. A., 2007, "Utilization of Alloy 693 in Metal Dusting Environments," *NACE International Corrosion 2007 Conference and Expo*, Nashville, TN, Mar. 11–15, Paper No. 07430.